A Central-Upwind Scheme for Nonlinear Water Waves Generated by Submarine Landslides

Alexander Kurganov[1] and Guergana Petrova[2]

[1] Mathematics Department, Tulane University, New Orleans, LA 70118
kurganov@math.tulane.edu
[2] Department of Mathematics, Texas A& M University, College Station, TX 77843
gpetrova@math.tamu.edu

We study a simple one-dimensional (1-D) toy model for landslides-generated nonlinear water waves. The landslide is modeled as a rigid bump translating down the side of the bottom while the water motion is modeled by the Saint-Venant system of shallow water equations. The resulting system is numerically solved using a well-balanced positivity preserving central-upwind scheme. The obtained numerical results are in good agreement with both the two-dimensional (2-D) incompressible flow numerical simulations and the experimental data.

1 Introduction

Landslides-generated water waves are of great interest to both ocean scientists and coastal and dams-keeping engineers. These landslides are natural phenomena that occur under certain conditions such as erosion, earthquakes, storms, heavy rainfalls, or water level fluctuations. In this paper, we study submarine landslides, which are capable of generating several types of long waves, including very powerful and destructive tsunami waves.

Modeling of landslides-generated water waves is based on two components: the description of the motion of the boundaries of the fluid domain and the equations governing the water motion. In this paper, we will consider a simple 1-D toy model for landslides-generated water waves. The landslide is modeled by a rigid bump that loses its equilibrium and begins to translate down the side of the bottom (see, e.g., [GW05, Hei92, HPH01]). The water motion is described by the Saint-Venant system of shallow water equations [SV1871], which is commonly accepted approximation governing long wave propagation in deep ocean as well as in near-shore regions, including inundation. In the 1-D case, the studied system is:

$$\begin{cases} h_t + (hu)_x = 0, \\ (hu)_t + \left(hu^2 + \dfrac{1}{2}gh^2\right)_x = -ghB_x, \end{cases} \tag{1}$$

where h is the fluid depth above the bottom, u is the velocity, g is the gravitational constant, and B represents the bottom elevation. Here, the only difference from the original Saint-Venant system is that the bottom topography function $B = B(x,t)$ is considered as a function not only of the space variable x, but also of the time t.

In the past few decades, a wide variety of reliable finite-volume methods for the Saint-Venant system has been developed. We refer the reader to [ABBLP04, JW05, KL02, KP, NPPN06, XS06] for just several recently proposed methods. In the context of tsunami waves propagation, the shallow water equations have been recently numerically solved in [GL06].

In order to accurately capture landslides-generated water waves, a numerical method should possess two very important properties. First, it should be well-balanced, that is, it should exactly preserve stationary steady states ($h + B \equiv$ const, $u \equiv 0$, $B_t \equiv 0$). Otherwise, even tiny perturbations of steady-state solutions may lead to "numerical storm", which would make the resolution of long water waves impossible due to their extremely small amplitude during the deep ocean propagation stage. The second important property of a good numerical method is the ability to preserve positivity of the water depth h. This feature is crucial for capturing water waves in near-shore regions and especially for resolving the inundation stage, when initially dry ($h = 0$) coastal areas flood after the wave hits the coastal line and then slowly drains out.

In this paper, we numerically solve the model (1) by the second-order central-upwind scheme from [KP]. This scheme is both well-balanced and positivity preserving. It is also capable of treating discontinuous bottom topographies. Furthermore, its extension to the case of time-dependent B is straightforward. We describe our method in §2 and present the obtained numerical results in §3.

2 Description of the Central-Upwind Scheme

In this section, we describe a second-order semi-discrete well-balanced positivity preserving central-upwind scheme for the system (1). This scheme belongs to the class of high-resolution non-oscillatory Godunov-type central schemes first introduced in [NT90]. Compared to upwind finite-volume methods, the central schemes enjoy the advantages of simplicity, robustness, and universality. However, the numerical dissipation of the staggered central schemes, for example the one from [NT90], is relatively large, which is especially prominent when the system is integrated for large times. In [KL07, KNP01, KT00], a new class of so-called semi-discrete central-upwind schemes has been introduced. These schemes enjoy all major advantages of Riemann-problem-solver-free central schemes, while their dissipation is lowered by incorporating some

upwind information about local speeds of propagation into the central setting. Central-upwind schemes have been applied to the Saint-Venant system in [KL02, KP].

For simplicity, we introduce a uniform grid $x_\alpha := \alpha\Delta x$, where Δx is a small spatial scale, and we denote by I_j the finite volume cells $I_j := [x_{j-\frac{1}{2}}, x_{j+\frac{1}{2}}]$.

We assume that at a certain time level t the computed solution is already available. We then replace the bottom topography function $B(\cdot,t)$ with its continuous piecewise linear approximation $\widetilde{B}(\cdot,t)$, consisting of the linear pieces that connect the points $(x_{j+\frac{1}{2}}, B_{j+\frac{1}{2}})$:

$$\widetilde{B}(x,t) = B_{j-\frac{1}{2}} + \left(B_{j+\frac{1}{2}} - B_{j-\frac{1}{2}}\right)\cdot\frac{x - x_{j-\frac{1}{2}}}{\Delta x}, \quad x_{j-\frac{1}{2}} \le x \le x_{j+\frac{1}{2}}, \tag{2}$$

where $B_{j+\frac{1}{2}} := (B(x_{j+\frac{1}{2}}+0,t) + B(x_{j+\frac{1}{2}}-0,t))/2$, which reduces to $B_{j+\frac{1}{2}} = B(x_{j+\frac{1}{2}},t)$ if $B(\cdot,t)$ is continuous at $x = x_{j+\frac{1}{2}}$. Note that $\{B_{j+\frac{1}{2}}\}$, like all other quantities reconstructed at time level t, depend on t, but we suppress this dependence in order to simplify the notation.

A central-upwind semi-discretization of (1) is the following system of ODEs:

$$\frac{d}{dt}\overline{\mathbf{U}}_j(t) = -\frac{\mathbf{H}_{j+\frac{1}{2}}(t) - \mathbf{H}_{j-\frac{1}{2}}(t)}{\Delta x} + \overline{\mathbf{S}}_j(t), \tag{3}$$

where $\overline{\mathbf{U}}_j(t)$ are approximations of the cell averages of the solution:

$$\overline{\mathbf{U}}_j(t) \approx \frac{1}{\Delta x}\int_{I_j}\mathbf{U}(x,t)\,dx, \quad \mathbf{U} := (h,q)^T,\ q := hu,$$

$\overline{\mathbf{S}}_j$ is an appropriate discretization of the cell averages of the source term $\mathbf{S} := (0, -ghB_x)^T$:

$$\overline{\mathbf{S}}_j(t) = \left(0, -g\overline{h}_j\frac{B_{j+\frac{1}{2}} - B_{j-\frac{1}{2}}}{\Delta x}\right)^T \approx \frac{1}{\Delta x}\int_{I_j}\mathbf{S}(\mathbf{U}(x,t), B(x,t))\,dx,$$

and the central-upwind numerical fluxes $\mathbf{H}_{j+\frac{1}{2}}$ are given by:

$$\mathbf{H}_{j+\frac{1}{2}} = \frac{a^+_{j+\frac{1}{2}}\mathbf{F}(\mathbf{U}^-_{j+\frac{1}{2}}) - a^-_{j+\frac{1}{2}}\mathbf{F}(\mathbf{U}^+_{j+\frac{1}{2}})}{a^+_{j+\frac{1}{2}} - a^-_{j+\frac{1}{2}}} + \frac{a^+_{j+\frac{1}{2}}a^-_{j+\frac{1}{2}}}{a^+_{j+\frac{1}{2}} - a^-_{j+\frac{1}{2}}}\left[\mathbf{U}^+_{j+\frac{1}{2}} - \mathbf{U}^-_{j+\frac{1}{2}}\right] \tag{4}$$

Here, $\mathbf{F}(\mathbf{U}) := (q, q^2/h + gh^2/2)^T$, and $\mathbf{U}^\pm_{j+\frac{1}{2}} = (h^\pm_{j+\frac{1}{2}}, q^\pm_{j+\frac{1}{2}})$ are the right/left-sided values of the piecewise linear reconstruction $\widetilde{\mathbf{U}} = (\widetilde{h}, \widetilde{q})$ at $x = x_{j+\frac{1}{2}}$. For the discharge q, we have:

$$\widetilde{q}(x) := \overline{q}_j + (q_x)_j(x - x_j), \quad x_{j-\frac{1}{2}} < x < x_{j+\frac{1}{2}}, \tag{5}$$

where the numerical derivative $(q_x)_j$ is (at least) first-order, componentwise approximation of $q_x(x_j,t)$, computed using a nonlinear limiter needed to ensure a non-oscillatory nature of the reconstruction (5). We use the generalized minmod limiter (see, e.g., [KT00, KNP01, LN03, NT90]):

$$(q_x)_j = \text{minmod}\left(\theta\frac{\overline{q}_j - \overline{q}_{j-1}}{\Delta x}, \frac{\overline{q}_{j+1} - \overline{q}_{j-1}}{2\Delta x}, \theta\frac{\overline{q}_{j+1} - \overline{q}_j}{\Delta x}\right), \quad \theta \in [1,2], \quad (6)$$

where the minmod function is defined as:

$$\text{minmod}(z_1, z_2, ...) := \begin{cases} \min_j\{z_j\}, & \text{if } \ z_j > 0 \ \ \forall j, \\ \max_j\{z_j\}, & \text{if } \ z_j < 0 \ \ \forall j, \\ 0, & \text{otherwise.} \end{cases}$$

The parameter θ can be used to control the amount of numerical diffusion present in the resulting scheme. In our numerical experiments, we have used $\theta = 1$.

As suggested in [KP], the well-balanced and positivity preserving property of the scheme is guaranteed if instead of reconstructing the water depth h, we perform a reconstruction for the fluid level $w := h + B$, and then use it to compute $h^{\pm}_{j+\frac{1}{2}} := w^{\pm}_{j+\frac{1}{2}} - B_{j+\frac{1}{2}}$. To this end, we first construct $\widetilde{w}$ in the same way as $\widetilde{q}$ was constructed in (5)–(6), with $\overline{w}_j := \overline{h}_j + (B_{j-\frac{1}{2}} + B_{j+\frac{1}{2}})/2$. Then, we correct the obtained $\widetilde{w}$ in the following two cases (see [KP] for details):

$$\text{if } \ w^-_{j+\frac{1}{2}} < B_{j+\frac{1}{2}}, \ \text{ then take } \ w^-_{j+\frac{1}{2}} := B_{j+\frac{1}{2}}, \ \ w^+_{j-\frac{1}{2}} := 2\overline{w}_j - B_{j+\frac{1}{2}},$$
$$\text{if } \ w^+_{j-\frac{1}{2}} < B_{j-\frac{1}{2}}, \ \text{ then take } \ w^-_{j+\frac{1}{2}} := 2\overline{w}_j - B_{j-\frac{1}{2}}, \ \ w^+_{j-\frac{1}{2}} := B_{j-\frac{1}{2}}.$$

This correction procedure guarantees that the resulting reconstruction $\widetilde{w}$ will stay above the piecewise linear approximant (2) of the bottom topography function. Therefore, the reconstructed values $h^{\pm}_{j+\frac{1}{2}}$ will be nonnegative.

To be able to accurately and efficiently treat (almost) dry regions, we also need to make a modification in the calculation of the velocities $u^{\pm}_{j+\frac{1}{2}}$ so that division by very small values of h is avoided. To achieve this goal, we follow [KP] and set:

$$u^{\pm}_{j+\frac{1}{2}} := \frac{\sqrt{2}\,h^{\pm}_{j+\frac{1}{2}}\,q^{\pm}_{j+\frac{1}{2}}}{\sqrt{\left(h^{\pm}_{j+\frac{1}{2}}\right)^4 + \max\left(\left(h^{\pm}_{j+\frac{1}{2}}\right)^4, \varepsilon\right)}}, \quad (7)$$

where ε is a small a-priori chosen positive number (in our numerical experiments, we have taken $\varepsilon = (\Delta x)^4$). Note that formula (7) can be replaced by an alternative desingularization strategy, but we selected this since (7) reduces to $u^{\pm}_{j+\frac{1}{2}} = q^{\pm}_{j+\frac{1}{2}}/h^{\pm}_{j+\frac{1}{2}}$ for large values of h. Next, we recompute the discharge q using:

$$q^{\pm}_{j+\frac{1}{2}} := h^{\pm}_{j+\frac{1}{2}} \cdot u^{\pm}_{j+\frac{1}{2}},$$

where $u^{\pm}_{j+\frac{1}{2}}$ are given by (7). Equipped with the values of $h^{\pm}_{j+\frac{1}{2}}$ and $u^{\pm}_{j+\frac{1}{2}}$, we compute the one-sided local speeds of propagation $a^{\pm}_{j+\frac{1}{2}}$, needed in (4):

$$a^+_{j+\frac{1}{2}} = \max\left\{u^+_{j+\frac{1}{2}} + \sqrt{gh^+_{j+\frac{1}{2}}}\,,\, u^-_{j+\frac{1}{2}} + \sqrt{gh^-_{j+\frac{1}{2}}}\,,\, 0\right\},$$
$$a^-_{j+\frac{1}{2}} = \min\left\{u^+_{j+\frac{1}{2}} - \sqrt{gh^+_{j+\frac{1}{2}}}\,,\, u^-_{j+\frac{1}{2}} - \sqrt{gh^-_{j+\frac{1}{2}}}\,,\, 0\right\}.$$

Finally, the fully-discrete central-upwind scheme is obtained by solving the system of ODEs (3) by a stable ODE solver of an appropriate order. In our numerical experiments, we have used the third-order strong stability preserving Runge-Kutta ODE solver from [GST01].

3 Numerical Results

In this section, we numerically solve a test problem from [Hei92], where both numerical and laboratory experiments were presented. The laboratory experiments were carried out in a $20 \times 0.55 \times 1.50$ m channel, where the water waves were generated by letting a triangular box slide down an inclined plane with a 45° slope. The shore is modeled by a second plane with a 15° slope. The box, a right isosceles triangle with 0.5 m sides, is initially 1 cm below the undisturbed free surface, and thus the bottom function at time $t = 0$ is given by (see Figure 1):

$$B(x,0) = \begin{cases} -\alpha x, & x \le 0, \\ -x, & 0 \le x \le 0.01, \\ -0.01, & 0.01 \le x \le 0.51, \\ -x, & 0.51 < x \le 1, \\ 0, & x \ge 1, \end{cases} \tag{8}$$

where the shore slope is $\alpha = \tan(\pi/12)$, and the initial condition is:

$$h(x,0) = \max\{1 - B(x,0), 0\}, \quad q(x,0) \equiv 0. \tag{9}$$

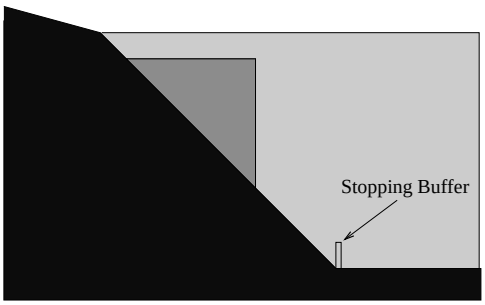

Fig. 1. Initial bottom topography

In [Hei92], the water motion is described by the 2-D incompressible Euler equations with free surface, which are numerically solved using the NASA-VOF2D code [TCMH85]. The numerical results reported in [Hei92] are comparable with the laboratory experiments.

Here, we obtain similar results, using the much simpler shallow water model (1) with an added friction term:

$$\begin{cases} h_t + q_x = 0, \\ q_t + \Big(\dfrac{q^2}{h} + \dfrac{1}{2}gh^2\Big)_x = -ghB_x - \kappa(h)u. \end{cases} \tag{10}$$

In our numerical experiments, we have taken the friction coefficient $\kappa(h) = 0.1/(1+10h)$.

We numerically solve the system (10) subject to the initial condition (9) and the initial bottom topography (8). Following [GW05], we describe the motion of the triangular box by the displacement of its center of mass from its initial position:

$$S(t) = \frac{\sqrt{2\pi(\gamma+1)}}{4}\ \ln\left(\cosh\left(\frac{t\sqrt{2g(\gamma-1)}}{(\gamma+1)\sqrt{\pi}}\right)\right). \tag{11}$$

Here, γ is the ratio of the bulk and water densities. In our numerical experiments, $\gamma = 1.925$ and the gravitational constant $g = 9.812$.

Equations (11) and (8) give a closed formula for the function $B(x,t)$ participating in the studied system (10), which is numerically solved by the central-upwind scheme. The cell average of the friction term in (10) is approximated using the mid-point rule, which affects neither the well-balanced nor the positivity preserving properties of our scheme.

The water surface, computed on both coarse (with $\Delta x = 1/25$) and fine (with $\Delta x = 1/200$) uniform grids is shown in Figures 2–3, where snapshots of the solution are taken at times $t = 0.5$, 1, 1.5, 2, 2.5, 3, 3.5, and 4. Clearly, the downward motion of the triangular box generates a nonlinear water wave. While the left counterpart of this wave hits the shore (see Figure 2, $t = 1.5$ and 2), the right counterpart gradually forms a stable "tsunami-like" shape that travels across the channel (see Figure 3, $t = 2.5$, 3, 3.5, and 4). Our results are in good agreement with the ones reported in [Hei92].

Acknowledgment: The research of A. Kurganov was supported in part by the NSF Grants # DMS-0310585 and DMS-0610430. The research of G. Petrova was supported in part by the NSF Grant # DMS-0505501.

References

[ABBLP04] Audusse, E., Bouchut, F., Bristeau, M.-O., Klein, R., Perthame, B.: A fast and stable well-balanced scheme with hydrostatic reconstruction for shallow water flows. SIAM J. Sci. Comput., **25**, 2050–2065 (2004).

[GL06] George, D.L., LeVeque, R.J.: Finite volume methods and adaptive refinement for global tsunami propagation and local inundation. Science of Tsunami Hazards, **24**, 319–328 (2006).

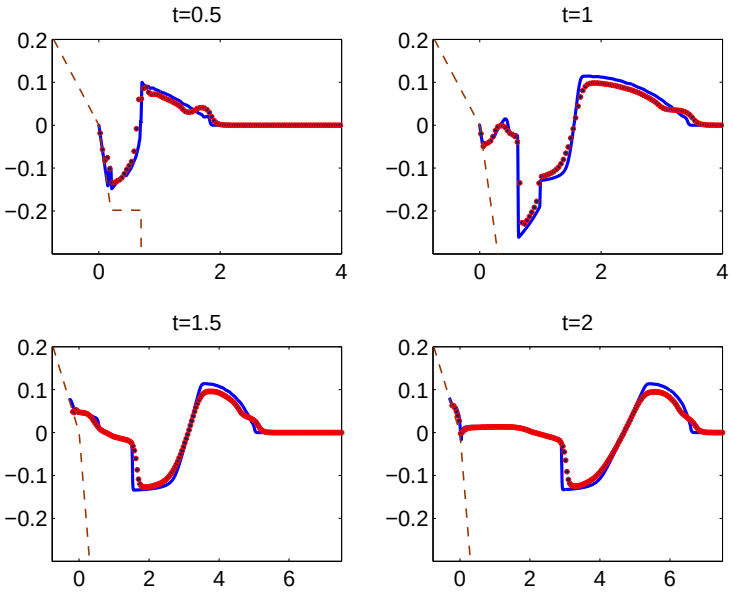

Fig. 2. Snapshots of the water surface $h + B$, computed on a coarser (dots) and a finer (solid line) grids. The dashed line represents the bottom

[GST01] Gottlieb, S., Shu, C.-W., Tadmor, E.: High order time discretization methods with the strong stability property. SIAM Rev., **43**, 89–112 (2001)

[GW05] Grilli, S., Watts, P.: Tsunami generation by submarine mass failure. I: Modeling, experimental validation, and sensitivity analyses. J. Waterway Port Coast. Oc. Eng., **131**, 283–297 (2005)

[Hei92] Heinrich, Ph.: Nonlinear water waves generated by submarine and areal landslides. J. Waterway Port Coast. Oc. Eng., **118**, 249–266 (1992)

[HPH01] Heinrich, Ph., Piatanesi, A., Hebert, H.: Numerical modelling of tsunami generation and propagation from submarine slumps: the 1998 Papua New Guinea event. Geophys. J. Int, **145**, 97–111 (2001)

[JW05] Jin, S., Wen, X.: Two interface-type numerical methods for computing hyperbolic systems with geometrical source terms having concentrations. SIAM J. Sci. Comput., **26**, 2079–2101 (2005)

[KL02] Kurganov, A., Levy, D.: Central-upwind schemes for the Saint-Venant system. M2AN Math. Model. Numer. Anal., **36**, 397–425 (2002)

[KL07] Kurganov, A., Lin, C.-T.: On the reduction of numerical dissipation in central-upwind schemes. Commun. Comput. Phys., **2**, 141–163 (2007)

[KNP01] Kurganov, A., Noelle, S., Petrova, G.: Semi-discrete central-upwind scheme for hyperbolic conservation laws and Hamilton-Jacobi equations. SIAM J. Sci. Comput., **23**, 707–740 (2001)

[KP] Kurganov, A., Petrova, G.: A second-order well-balanced positivity preserving central-upwind scheme for the Saint-Venant system. submitted to Commun. Math. Sci.

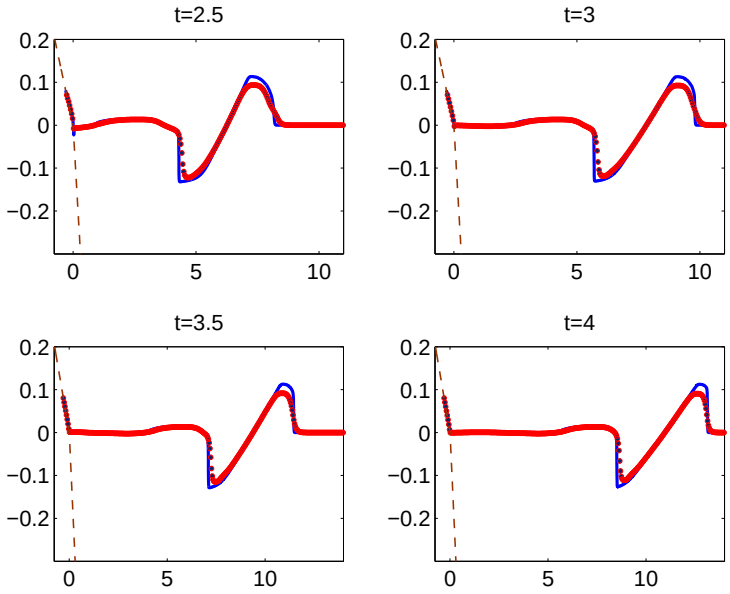

Fig. 3. The same as Figure 2, but at later times

[KT00] Kurganov, A., Tadmor, E.: New high-resolution central schemes for nonlinear conservation laws and convection-diffusion equations. J. Comput. Phys., **160**, 241–282 (2000)

[LN03] Lie, K.-A., Noelle, S.: On the artificial compression method for second-order nonoscillatory central difference schemes for systems of conservation laws. SIAM J. Sci. Comput., **24**, 1157–1174 (2003)

[NT90] Nessyahu, H., Tadmor, E.: Non-oscillatory central differencing for hyperbolic conservation laws. J. Comput. Phys., **87**, 408–463 (1990)

[NPPN06] Noelle, S., Pankratz, N., Puppo, G., Natvig, J.: Well-balanced finite volume schemes of arbitrary order of accuracy for shallow water flows. J. Comput. Phys., **213**, 474–499 (2006)

[ORM00] Ortiz, M., Gomez-Reyes, E., Velez-Munoz, H.: A fast preliminary estimation model for transoceanic tsunami propagation. Geofisica Internatcional, **39**, 207–220 (2000)

[SV1871] de Saint-Venant, A. J. C.: Thèorie du mouvement non-permanent des eaux, avec application aux crues des rivière at à l'introduction des marèes dans leur lit. C.R. Acad. Sci. Paris, **73**, 147–154 (1871)

[TCMH85] Torrey, M.D., Cloutman, L.D., Mjolness, R.C., Hirt, C.W.: NASA-VOF2D: A computer program for incompressible flows with free surfaces. Report LA-10612-MS, Los Alamos Nat. Lab.,Los Alamos, N.M. (1985)

[XS06] Xing, Y., Shu, C.-W.: A new approach of high order well-balanced finite volume WENO schemes and discontinuous Galerkin methods for a class of hyperbolic systems with source terms, Commun. Comput. Phys., **1**, 100–134 (2006)